J|A|C|S
ARTICLES
Published on Web 04/27/2004

Marcus Theory of Outer-Sphere Heterogeneous Electron Transfer Reactions: Dependence of the Standard Electrochemical Rate Constant on the Hydrodynamic Radius from High Precision Measurements of the Oxidation of Anthracene and Its Derivatives in Nonaqueous Solvents Using the High-Speed Channel Electrode

Antony D. Clegg, Neil V. Rees, Oleksiy V. Klymenko, Barry A. Coles, and Richard G. Compton*

Contribution from the Physical and Theoretical Chemistry Laboratory, Oxford University, South Parks Road, Oxford OX1 3QZ, United Kingdom

Received January 12, 2004; E-mail: richard.compton@chemistry.ox.ac.uk

Abstract: The validity of Marcus theory for outer-sphere heterogeneous electron transfer for the electrooxidation of a range of anthracene derivatives in alkyl cyanide solvents is investigated. The precision measurement of these fast electron transfers ($k_0 \geq 1$ cm s^{-1}) is achieved by use of the high-speed channel electrode and, where necessary, fast-scan cyclic voltammetry. First, the solvent effect on the rate of electron transfer is studied by considering the first oxidation wave of 9,10-diphenylanthracene in the alkyl cyanide solvents: acetonitrile, propionitrile, butyronitrile, and valeronitrile. Second, the variation of k_0 for a series of substituted anthracenes is investigated by analyzing the voltammetric response of the one-electron oxidations of 9-phenylanthracene, 9,10-dichloroanthracene, 9-chloroanthracene, 9,10-dicyanoanthracene, 9-cyanoanthracene, 9-nitroanthracene, 9,10-diphenylanthracene, and anthracene in acetonitrile. It is shown that the rate of electron transfer of a single compound in different alkyl cyanides is determined by the longitudinal dielectric relaxation properties of the solvent, while differences in rate between the substituted anthracenes in acetonitrile can be *quantitatively* rationalized by considering their relative hydrodynamic radii. This makes possible the accurate prediction of electron-transfer rates for a molecule by interpolation of rate constants known for related molecules.

Introduction

The theory of electrochemical electron transfer has been expanded greatly since the early work of Marcus.[1−7] These developments have been in directions such as: outer- and inner-sphere transfers,[8,9] the application of quantum theory, consideration of the role of electrode material and double layer effects (for heterogeneous transfers),[10−12] the nature of the donor and acceptor species (for homogeneous transfers), and especially the role of the solvent and solvent dynamics.[13−21] These extensions to the original basic theory have all sought to more closely fit the experimentally observed rates, with varying degrees of success. A great deal of experimental work has been performed in the context of homogeneous electron transfer (including self-exchange reactions), due to practical convenience.[7] The field of heterogeneous electron transfer, i.e., electron transfer to or from an electrode, has been relatively neglected as a result. In both cases, experiment has generally confirmed Marcus theory, at least qualitatively.[7] In recent years there have been more efforts focused on heterogeneous transfers,[22−26] and this paper concentrates exclusively on this.

Electron-transfer reactions are usually divided between inner- and outer-sphere reactions depending on the degree of interaction of the redox species with the electrode. In the former case, the redox species penetrates the inner Helmholtz layer so that direct contact is made with the electrode surface, whereas outer-

(1) Marcus, R. A. *J. Chem. Phys.* **1956**, *24*, 966.
(2) Marcus, R. A. *J. Chem. Phys.* **1956**, *24*, 979.
(3) Marcus, R. A. *J. Chem. Phys.* **1957**, *26*, 867.
(4) Marcus, R. A. *J. Phys. Chem.* **1963**, *67*, 853.
(5) Marcus, R. A. *J. Chem. Phys.* **1965**, *43*, 679.
(6) Dogonadze, R. R.; Kuznetsoz, A. M. *Prog. Surf. Sci.* **1975**, *6*, 1.
(7) Weaver, M. J. In *Comprehensive Chemical Kinetics*; Compton, R. G., Ed.; Elsevier: Amsterdam, The Netherlands, 1987; Vol. 27, p 1.
(8) Chandra, A. *J. Chem. Phys.* **1999**, *110*, 1569.
(9) Hynes, J. T. *J. Phys. Chem.* **1986**, *90*, 3701.
(10) Fawcett, W. R. *Electrochim. Acta* **1997**, *42*, 833.
(11) Mohilner, D. M. *J. Phys. Chem.* **1969**, *75*, 2652.
(12) Smith, B. B.; Hynes, J. T. *J. Chem. Phys.* **1993**, *99*, 6517.
(13) Calef, D. F.; Wolynes, P. G. *J. Chem. Phys.* **1983**, *78*, 470.
(14) Calef, D. F.; Wolynes, P. G. *J. Phys. Chem.* **1983**, *87*, 3387.
(15) Tachiya, M. *Radiat. Phys. Chem.* **1996**, *47*, 43.
(16) Leite, V. B. P.; Onuchic, J. N. *J. Phys. Chem.* **1996**, *100*, 7680.
(17) Leite, V. B. P. *J. Chem. Phys.* **1999**, *110*, 10067.
(18) Hartnig, C.; Koper, M. T. M. *J. Chem. Phys.* **2001**, *115*, 8540.
(19) Samanta, A.; Ghosh, S. K. *Chem. Phys.* **1997**, *214*, 61.
(20) Hilczer, M.; Tachiya, M. *J. Mol. Liq.* **1995**, *64*, 113.
(21) Kim, H. J.; Hynes, J. T. *J. Phys. Chem.* **1990**, *94*, 2736.
(22) Zhang, X.; Leddy, J.; Bard, A. J. *J. Am. Chem. Soc.* **1985**, *107*, 3719.
(23) Kojima, H.; Bard, A. J. *J. Am. Chem. Soc.* **1975**, *97*, 6317.
(24) Garreau, D.; Savéant, J. M.; Tessier, D. *J. Phys. Chem.* **1979**, *83*, 3003.
(25) Savéant, J. M.; Tessier, D. *Faraday Discuss. Chem. Soc.* **1982**, *74*, 57.
(26) Amatore, C.; Savéant, J. M.; Tessier, D. *J. Electroanal. Chem.* **1983**, *146*, 37.

sphere reactions maintain the integrity of the molecule and its solvation shell such that no such direct interaction exists.[7]

Outer-sphere electron transfer is usually discussed in terms of an "encounter pre-equilibrium" model[7] involving the formation of a precursor complex between the reactant molecule and the electrode surface, with an equilibrium constant, K_p, and free energy of activation $\Delta G^{\ddagger}$. Hence, k_0 can be expressed as

$$k_0 = \kappa_{el} K_p \upsilon_n \exp\left(\frac{-\Delta G^{\ddagger}}{RT}\right) \quad (1)$$

where ν_n (s^{-1}) is the nuclear frequency factor (the frequency of crossing the free energy barrier) and κ_{el} is the electronic transmission coefficient (the probability of electron tunneling in the transition state).[7,27,28]

It has been shown that solvent reorientation dynamics can have a dominating effect upon the heterogeneous rate constant.[28−33] If the reaction free energy is zero, and the "weak overlap" limit is assumed (i.e., the electronic coupling is small), then[28]

$$\upsilon_n = {\tau_L}^{-1}\left(\frac{\Delta G^{\ddagger}}{4\pi RT}\right)^{1/2} \quad (2)$$

where τ_L is defined as $\tau_L = \tau_D \epsilon_\infty/\epsilon_s$, τ_D is the experimental Debye relaxation time, and ϵ_∞ and ϵ_s are the high frequency and static dielectric permittivities, respectively.[7]

Several studies have sought to investigate this relationship, by measuring the electron-transfer rates in a variety of different solvents.[31−33] These have confirmed a linear relationship between k_0 and ${\tau_L}^{-1}$ and also indicate the presence of an outer-sphere rather than inner-sphere pathway. However, relatively little work has been directed at using eq 1 to interpret trends in reaction rates. If this is to be done, the method used to measure the rates of electron transfer needs to be proven as reliable and precise. The demands placed upon the method are exacerbated if the reaction rates are fast.

In general, there are steady-state and transient methods available to the experimentalist for making measurements of electron transfers. There have been several reviews on the subject of measurement of fast electrochemical kinetics,[34−37] but in essence the transient methods employed are based on fast-scan cyclic voltammetry,[38−41] whereas the steady-state methods depend either on diffusion to ever decreasingly sized disk electrodes[42,43] or on hydrodynamic methods.[44−46] Great advances have been made in instrumentation in recent years to facilitate the use of high voltage scan rates, by reducing the problems of *iR* losses through on-line compensation circuitry[47−49] and shielded microelectrodes to reduce capacitative currents.[50,51] However, the successful use of fast scan cyclic voltammetry is reliant on a high degree of experimental skill and the analysis of voltammetry is complicated by the residual distortions of *iR* and capacitative effects.[36] Obtaining repetitively consistent data is therefore often difficult. Steady-state voltammetry would appear, therefore, to offer the advantage of not having these complications. However, the use of ultramicroelectrodes and nanotrodes is complicated by their construction and suitability for use in organic solvents, as many are fabricated using epoxy resins that swell or dissolve in nonaqueous solvents. Even if the electrode is suitable for use, there can be a problem in measuring the very small currents produced with sufficient accuracy to analyze successfully. Since most analyses of the sigmoidal response of ultramicrodisks are based on the method of Mirkin and Bard,[52] it is then necessary to obtain very smooth voltammograms on the nanoamp scale to extract the required quartile potentials. It is therefore not unusual for a relatively large error to be compounded into these measurements.

Perhaps of all the steady-state methods, hydrodynamic electrodes offer the best means in principle of measuring fast kinetics. Experimentally, the optimal systems are the wall-tube or channel electrodes, which achieve the high mass transport coefficients needed to measure electron-transfer rates above 1 cm s^{-1}. The wall-tube, or microjet, electrode has been developed and used by Unwin et al.[53−56] for several studies, including the measurement of the electron transfer of the hexacyanoferrate-(II/III) redox couple to be 0.76 cm s^{-1}, using the Mirkin and Bard analysis method.[54] However, the microjet has not yet been used to access the faster rates of electron transfer expected in nonaqueous solvents, such as acetonitrile. Furthermore, in a recent study, the authors showed there were inherent problems in attempting to use a high-flow microjet in solvents less viscous than water.[57] The channel electrode has been used in several studies for the measurement of fast kinetics[58,59] and specifically electron transfer,[60,61] and a rigorous method has recently been developed for analysis of experimental data that provides a consistent and precise means of extracting the values of k_0, α,

(27) Marcus, R. A. *Int. J. Chem. Kinet.* **1981**, *13*, 865.
(28) Opallo, M. *J. Chem. Soc., Faraday Trans. 1* **1986**, *82*, 339.
(29) Fawcett, W. R.; Opallo, M.*J. Electroanal. Chem.* **1993**, *349*, 273.
(30) Gennett, T.; Milner, D. F.; Weaver, M. J. *J. Phys. Chem.* **1985**, *89*, 2787.
(31) Fernandez, H.; Zon, M. A. *J. Electroanal. Chem.* **1990**, *283*, 251.
(32) Fernandez, H.; Zon, M. A *J. Electroanal. Chem.* **1992**, *332*, 237.
(33) Moressi, M. B.; Zon, M. A.; Fernandez, H. *Electrochim. Acta* **2000**, *45*, 1669.
(34) Heinze, J. *Angew. Chem., Int. Ed. Engl.* **1993**, *23*, 1268.
(35) Forster, R. F. In *Encyclopedia of Analytical Chemistry*; Meyers, R. A., Ed.; Wiley: Chichester, 2000; Vol. 11, p 10142.
(36) Andrieux, C. P.; Hapiot, P.; Savéant, J.-M. *Chem. Rev.* **1990**, *90*, 723.
(37) Wightman, R. M.; Wipf, D. O. In *Electroanalytical Chemistry*; Bard, A. J., Ed.; Marcel Dekker: New York, 1989; Vol. 15, p 267.
(38) Garreau, D.; Hapiot, P.; Savéant, J.-M. *J. Electroanal. Chem.* **1989**, *272*, 1.
(39) Wipf, D. O.; Wightman, R. M. *Anal. Chem.* **1988**, *60*, 2460.
(40) Howell, J. O.; Wightman, R. M. *Anal. Chem.* **1984**, *56*, 524.
(41) Wightman, R. M.; Wipf, D. O. *Acc. Chem. Res.* **1990**, *23*, 64.
(42) Morris, R. B.; Franta, D. J.; White, H. S. *J. Phys. Chem.* **1987**, *91*, 3559.
(43) Chen, S.; Kucernak, A. *J. Phys. Chem. B* **2002**, *106*, 9396.
(44) Brett, C. M. A.; Oliveira Brett, A. M. C. F. In *Comprehensive Chemical Kinetics*; Bamford, C. H., Compton, R. G., Eds.; Elsevier: Amsterdam, The Netherlands, 1986; Vol. 26, p 355.
(45) Eklund, J. C.; Bond, A. M.; Alden, J. A.; Compton, R. G. *Adv. Phys. Org. Chem.* **1999**, *32*, 1.
(46) Macpherson, J. V.; Simjee, N.; Unwin, P. R. *Electrochim. Acta* **2001**, *47*, 29.
(47) Amatore, C.; Lefrou, C.; Pfluger, F. *J. Electroanal. Chem.* **1989**, *270*, 43.
(48) Amatore, C.; Maisonhaute, E.; Simmonneau, G. *Electrochem. Commun.* **2000**, *2*, 81.
(49) Amatore, C.; Maisonhaute, E.; Simmonneau, G. *J. Electroanal. Chem.* **2000**, *486*, 141.
(50) P. Tschuncky, P.; Heinze, J. *Anal. Chem.* **1995**, *67*, 4020.
(51) Nomura, S.; Nozaki, K.; Okazaki, S. *Anal. Chem.* **1991**, *63*, 2665.
(52) Mirkin, M. V.; Bard, A. J. *Anal. Chem.* **1992**, *64*, 2293.
(53) Macpherson, J. V.; Marcar, S.; Unwin, P. R. *Anal. Chem.* **1994**, *66*, 2175.
(54) Macpherson, J. V.; Beeston, M. A.; Unwin, P. R. *J. Chem. Soc., Faraday Trans. 1* **1995**, *91*, 899.
(55) Martin, R. D.; Unwin, P. R. *J. Electroanal Chem.* **1995**, *397*, 325.
(56) Macpherson, J. V.; Unwin, P. R. *Anal. Chem.* **1999**, *71*, 4642.
(57) Rees, N. V.; Klymenko, O. V.; Coles, B. A.; Compton, R. G. *J. Phys. Chem.* **2003**, *107*, 13649.
(58) Rees, N. V.; Dryfe, R. A. W.; Cooper, J. A.; Coles, B. A.; Compton, R. G.; Davies, S. G.; McCarthy, T. D. *J. Phys. Chem.* **1995**, *99*, 7096.
(59) Coles, B. A.; Dryfe, R. A. W.; Rees, N. V.; Compton, R. G.; Davies, S. G.; McCarthy, T. D. *J. Electroanal Chem.* **1996**, *411*, 121.
(60) Rees, N. V.; Alden, J. A.; Dryfe, R. A. W.; Coles, B. A.; Compton, R. G. *J. Phys. Chem.* **1995**, *99*, 14813.
(61) Rees, N. V.; Klymenko, O. V.; Coles, B. A.; Compton, R. G. *J. Electroanal. Chem.* **2002**, *534*, 151.

and E_f^0 simultaneously from the sigmoidal waveshape.[61] This method has enabled k_0 values up to 3 cm s^{-1} to be routinely measured[61] under steady-state conditions without the complications of charging currents and *iR* losses.

The aim of this paper is to investigate the *quantitative* applicability of the Marcus theory described above for *fast* outer-sphere heterogeneous electron transfers using the high-speed channel electrode (HSChE). This is to be achieved in two parts. First, the solvent effect on the rate of electron transfer is studied by considering the one-electron oxidations of 9,10-diphenylanthracene (DPA) in the alkyl cyanide (RCN) solvents acetonitrile (MeCN), propionitrile (EtCN), butyronitrile (PrCN), and valeronitrile (BuCN) with reference to eq 2. Second, the variation of k_0 for a series of substituted anthracenes is investigated by measuring the first oxidation wave of 9-phenylanthracene (PA), 9,10-dichloroanthracene (DCA), 9-chloroanthracene (CA), 9,10-dicyanoanthracene (DCNA), 9-cyanoanthracene (CNA), 9-nitroanthracene (NA), anthracene (AN), and DPA in acetonitrile, with analysis by means of an expanded form of eq 1. Novelly, the results can be successfully understood in terms of this equation by using the hydrodynamic radius to be the molecular dimension used.

Experimental Section

Reagents. Chemical reagents used were PA and DPA (both Aldrich, 98%), CA (Lancaster, 97%), DCA (Aldrich, 98%), CNA (Aldrich, 97%), DCNA (Kodak, 97%), NA (Aldrich, 97%), AN (Aldrich, 97%), supporting electrolyte tetrabutylammonium perchlorate (TBAP; Fluka, Puriss electrochemical grade, >99%), MeCN (Fisher scientific, "dried distilled", >99.99%), EtCN (Fluka, purum >99%), PrCN (Aldrich, 98%), and BuCN (Fluka, puriss >99%). These were the highest grades available and were used without further purification. Solvents were stored over molecular sieves (Linde 5 Å, Aldrich) for several hours prior to use. All solutions contained 0.10 M TBAP as supporting electrolyte and were degassed with argon (Pureshield Argon, BOC gases, UK). All experiments were conducted at a temperature of 294 ± 1 K.

Instrumentation. The high-speed channel electrode (HSChE) and pressurized apparatus have been described previously[58−60] and are shown schematically in Figures 1 and 2. Extremely high flow rates across a microband electrode are achieved by pressurizing a chamber containing the solution and electrode assembly up to 1.5 atm. The solution flows through a specially designed flow-cell (width, $d = 0.200$ cm and height, $2h = 126$ μm) and out through one of three capillaries of varying internal bore size, to the exit which is at ambient atmospheric pressure. In this way, volume flow rates of between 0.10 and 3.2 cm^3 s^{-1} (corresponding to linear flow velocities close to the electrode of 0.7 to 20 m s^{-1}) can be achieved. At the highest volume flow rates, the Reynolds number, *Re*, given by[44]

$$Re = \frac{3V_f}{2hdv} \tag{3}$$

can attain values of 9×10^3 under well-defined laminar conditions. The apparatus has been designed such that these *Re* numbers are present for only ca. 2 mm before the electrode. This length is less than the "lead in" length required for turbulence to develop, for example, at the highest volume low rates a "lead in" of ca. 4 mm is required for turbulence to set in. This "lead in" length can be estimated by

$$x_t \approx \frac{4h(3.04 \times 10^5)}{Re(1 + \eta_t)} \tag{4}$$

with $\eta_t = (v_0 - \bar{v})/\bar{v}$, where v_0 and $\bar{v}$ are the axial and mean velocities,

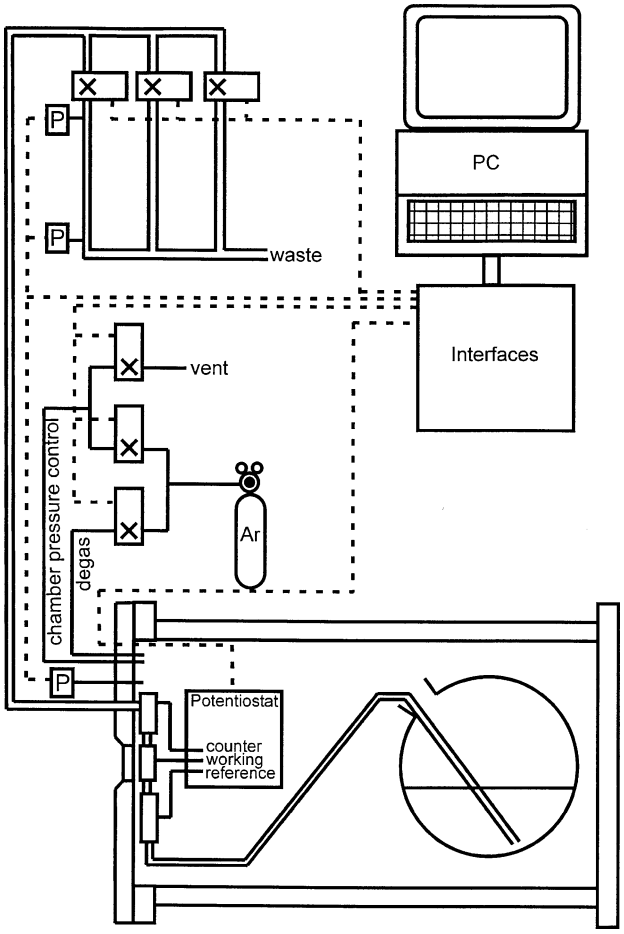

Figure 1. Schematic diagram of the HSChE.

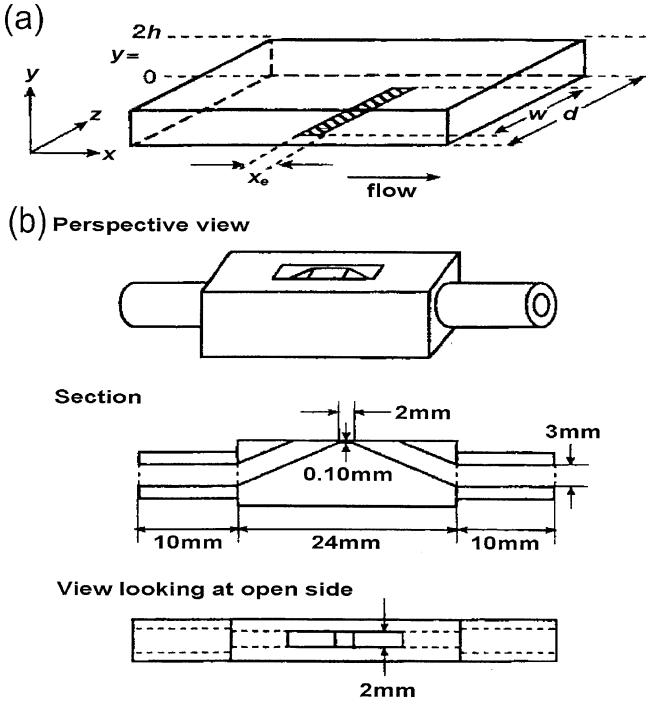

Figure 2. Diagram of the channel cell and microband electrode showing the geometrical parameters.

respectively.[58] Voltammograms are measured by means of an in-built potentiostat capable of providing voltage scan rates of between 1 mV s^{-1} and 5 V s^{-1} and detecting currents above 10 nA with no filtering.

For the experiments described here, a scan rate of 400 mV s^{-1} was employed. The control of solution flow and voltammogram measurement is entirely controlled by computer.

The "fast scan" potentiostat used for microdisk voltammetry was capable of achieving a voltage scan rate of up to 2×10^6 V s^{-1} and was used with minimum filtering. This potentiostat is identical to that described and utilized by Amatore and co-workers[48,49] and is capable of achieving ohmic drop compensation by means of an internal positive feedback circuit. The potential was applied with a TTi TG1304 programmable function generator (Thurlby Thandar Instruments Ltd, Huntingdon, Cambs, UK) and the current recorded with a Tektronix TDS 3032 oscilloscope (300 MHz band-pass, 2.5 GS/s).

Computer programs were written in DELPHI V6 PROFESSIONAL (Borland Software Corporation, Scotts Valley, CA) and run on a Pentium 4 computer, which was also used for data analysis.

Microelectrodes. Microband electrodes of length (x_e) 12.5μm were fabricated by fusing a strip of platinum foil (99.95%, Johnson Matthey plc, London, UK) into freshly cleaved soda glass at a temperature of 935 K for 3.5 h. One side of the glass was then ground using a diamond lapping wheel and polished using various grades of alumina slurry (BDH) from 3 μm down to 0.25 μm on glass and soft lapping pads (Kemet Ltd, UK) to a mirror finish to form the working face, and the other side was connected to a copper strip to provide an electrical contact. The electrode widths (w), as measured by microscope, were 0.100 cm.

For the fast scan cyclic voltammetry experiments, the working electrode was a platinum microdisk of diameter ($2r_d$) 12.5 μm fabricated by sealing a platinum microwire into capillary soda-glass. The microwire was placed alongside a thicker platinum connecting wire inside the capillary before being fused in a gas flame. The working face was ground and polished as described above, and the connecting wire was secured to provide a stable contact.[37] In both cases, the electrode dimensions were confirmed by measurements made using a literature methodology for electrochemical calibration.[62] The electrodes were cleaned with ultrapure water and approximately 30% nitric acid and then polished using alumina lapping compounds of decreasing size from 3 μm down to 0.25 μm on soft lapping pads, finally rinsed in ultrapure water, then dried carefully and stored under MeCN before use. The counter electrode was a smooth, bright, platinum mesh, and a silver wire (99.95%, Johnson Matthey plc, London, UK) was used as a quasi-reference electrode. Fast scan cyclic voltammetry was performed within a Faraday cage to reduce electrical noise.

Analysis of Steady-State Voltammetry. The experimental data were analyzed according to a previously reported method.[61] Steady-state voltammograms were normalized and then input into a program that calculated the "normalized" voltammogram of (I/I_{lim}) vs E for a selected range of α, k_0, and E_f^0 values. The quasi-reversible electron transfer to be simulated can be treated as

$$A - e^- \underset{k_f}{\overset{k_b}{\rightleftharpoons}} B$$

where

$$k_f = k_0 \exp\left(\frac{(1-\alpha)F}{RT}(E - E_f^0)\right) = k_0 \exp\{(1-\alpha)\theta\} \quad (5)$$

$$k_b = k_0 \exp\left(-\frac{\alpha F}{RT}(E - E_f^0)\right) = k_0 \exp(-\alpha\theta) \quad (6)$$

and its simulation was achieved by using analytical theory developed from initial work by Blaedel and Klatt[63,64] in the context of a tubular electrode. A transformation of their cylindrical coordinates into the rectangular analogues appropriate to the channel electrode gives the following result:[60,61]

$$\frac{i}{i_{rev}} = 1 - 2u + 2u^2 \ln(1 + u^{-1}) \quad (7)$$

where

$$u = \frac{0.6783 D_B^{2/3} (3V_f/4dx_e h^2)^{1/3}}{k_0[\exp[-(1-\alpha)\theta] + (D_A/D_B)^{2/3} \exp(\alpha\theta)]} \quad (8)$$

and

$$i_{rev} = \frac{0.925 nFw[A]_{bulk} (x_e D_A)^{2/3} (h^2 d)^{-1/3} V_f^{1/3}}{1 + (D_A/D_B)^{2/3} \exp(-\theta)} \quad (9)$$

where V_f is the volume flow rate, $[A]_{bulk}$ is the bulk concentration of the electroactive species, D_i is the diffusion coefficient of species i, and the geometrical parameters are as given in Figure 2. The quantity i_{rev} is the current that would flow if the electrode kinetics were reversible.

These approximate results have been compared to numerical simulations of the relevant mass-transport equations and associated boundary conditions using the backward implicit finite difference method;[60] the analytical solution described above was found to be in very good agreement with the numerical solution at the range of flow rates employed in the present study.[60]

For each simulated voltammogram, a mean scaled absolute deviation (MSAD) given by

$$\mathrm{MSAD}(\alpha, k_0, E_f^0) = \sum_{k=1}^{N} \frac{|I_{exp}(E_k) - I_{th}(\alpha, k_0, E_k - E_f^0)|}{I_{exp}(E_k)} \quad (10)$$

was calculated as the sum of the differences between each simulated point (I_{th}) and each experimental point (I_{exp}). Here, E_k, $k = 1, ..., N$ are the potentials of the experimental data points under analysis, and N is typically above 20. Each simulated voltammogram was therefore awarded its own MSAD value and this enabled a minimum to be found by a Direct Search Method—corresponding to the optimum values of α, k_0, and E_f^0.[61] Contour plots of MSAD as a function of α and k_0 and as a function of k_0 and E_f^0 were produced showing the existence of a single minimum in every case (see Supporting Information).

Results and Discussion

The HSChE provides a reliable means of obtaining fast electrochemical kinetic information to a high level of precision under steady-state conditions, and we therefore employed the system to measure the heterogeneous electron-transfer rate constants (k_0) for the following compounds. First, the solvent effect on the rate of electron transfer was investigated by considering the one-electron oxidation of DPA in the alkyl cyanide (RCN) solvents MeCN, EtCN, PrCN, and BuCN. Second, the variation of k_0 within a series of similar compounds was investigated by measuring the one-electon oxidations of PA, DCA, CA, DCNA, CNA, NA, and DPA in acetonitrile.

Oxidation of DPA in Alkyl Cyanides. A solution containing 0.93 mM DPA and 0.10 M TBAP in EtCN was introduced into the pressure chamber of the HSChE apparatus fitted with the 12.5 μm Pt microband electrode and an initial pressure set in order to fill the system. A linear sweep voltammogram was then recorded at a scan rate of 400 mV s^{-1}, and an arbitrary flow rate (0.51 cm^3 s^{-1} in this case) which yielded an effective steady-

(62) Brookes, B. A.; Lawrence, N. S.; Compton, R. G. *J. Phys. Chem. B* **2000**, *104*, 11258.
(63) Blaedel, W. J.; Klatt, L. N. *Anal. Chem.* **1966**, *38*, 879.
(64) Klatt, L. N., Blaedel, W. J. *Anal. Chem.* **1967**, *39*, 1065.

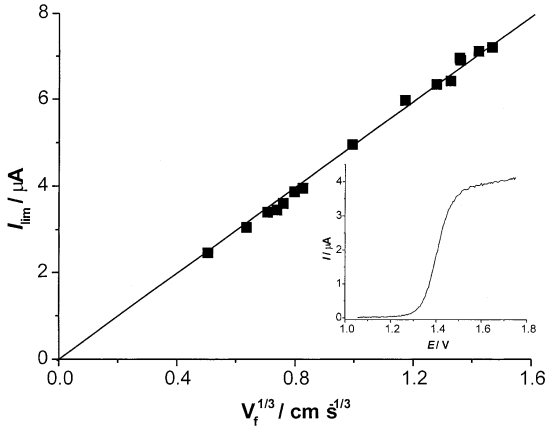

Figure 3. Levich plot for 0.93 mM DPA in EtCN/0.1M TBAP (gradient $= 4.10 \times 10^{-6}$; $R^2 = 0.996$). Inset shows a typical steady-state linear-sweep voltammogram ($V_f = 0.51$ cm^3 s^{-1}).

state response, enabling a limiting current (I_{lim}) to be measured for the first oxidation wave as shown in the inset in Figure 3. This was repeated for a range of chamber pressures from 20 to 150 kPa using a combination of capillary choice and pressure to access a range of volume flow rates (V_f) from 0.15 to 3.10 cm^3 s^{-1}. Figure 3 shows a "Levich plot" of measured limiting currents against $V_f^{1/3}$, according to the Levich equation[65] for channel flow cells:

$$I_{lim} = 0.925nFw[A]_{bulk}(x_eD)^{2/3}\left(\frac{V_f}{h^2d}\right)^{1/3} \qquad (11)$$

where n, F, and $[A]_{bulk}$ have their usual meaning, V_f is the volume flow rate, and the other terms represent the geometry of the channel cell and electrode as shown in Figure 2. The gradient of this plot was used to obtain a value for the diffusion coefficient of DPA in EtCN of $(1.18 \pm 0.05) \times 10^{-5}$ cm^2 s^{-1}, which compares well with an estimated value of 1.2×10^{-5} cm^2 s^{-1} as calculated from the Wilke−Chang expression:[66]

$$D \approx \frac{(7.4 \times 10^{-8})T\sqrt{\phi m_s}}{\eta\sigma^{0.6}} \qquad (12)$$

where T is the absolute temperature, ϕ is the solvent affinity factor (unity for aprotic solvents), m_s is the molecular mass of the solvent, η is the solvent viscosity, and σ the molecular volume.[66]

The current response for each voltammogram was normalized by division by the respective I_{lim} and the middle 60% of the wave was plotted against the potential to produce a "normalized voltammogram". These data were then input into the computer program described above and optimum values of k_0, α, and E_f^0 were calculated simultaneously for each voltammogram and the mean values taken. Figure 4 shows the 3-dimensional surface plots for k_0, E_f^0, and k_0, α respectively, as they vary independently with MSAD. The plots show single minima, demonstrating that there is only one set of optimized values.

The same procedure was repeated for the oxidation of DPA in PrCN (0.63 mM) and BuCN (1.02 mM) so that the kinetic information could be used in conjunction with the DPA in MeCN data obtained previously.[67] In all cases, excellent Levich

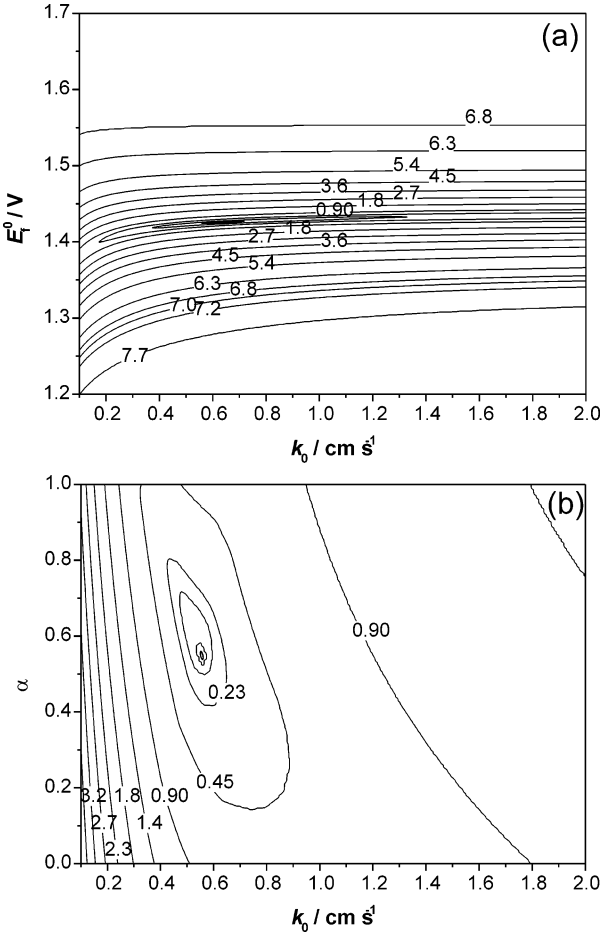

Figure 4. Contour plots for DPA in EtCN, with $V_f = 2.86$ cm^3 s^{-1}, showing (a) k_0 vs E_f^0 and (b) k_0 vs α. Numbers shown on contours are the MSAD values.

Table 1. Kinetic Parameters Obtained for the Oxidation of DPA in Alkyl Cyanides

solvent	$D \times 10^5$/cm^2 s^{-1}	k_0/cm s^{-1}	a	E_f^0/V (vs Ag)
MeCN[62]	1.40 ± 0.11	0.94 ± 0.16	0.53 ± 0.02	1.400 ± 0.010
EtCN	1.18 ± 0.05	0.61 ± 0.12	0.54 ± 0.03	1.396 ± 0.044
PrCN	0.95 ± 0.10	0.32 ± 0.07	0.49 ± 0.01	1.397 ± 0.024
BuCN	0.83 ± 0.10	0.23 ± 0.03	0.54 ± 0.03	1.319 ± 0.004

plots were obtained (with $R^2 \geq 0.996$) which yielded values for the respective diffusion coefficients that were all in good agreement with those predicted by the Wilke−Chang method. The analysis confirmed that these compounds exhibit a simple one-electron oxidation, and the kinetic parameters derived are shown in Table 1 (mean ± standard deviation).

For the case where the same molecule is studied in a homologous series of solvents, if we assume that terms in eq 1 such as κ_{el}, K_p, and $\Delta G^{\ddagger}$ are approximately unchanged in each solvent, the resulting relation is

$$k_0 = A\tau_L^{-1} \qquad (13)$$

where

$$A = \kappa_{el}K_p\left(\frac{\Delta G^{\ddagger}}{4\pi RT}\right)^{1/2}\exp\left(\frac{-\Delta G^{\ddagger}}{RT}\right)$$

(65) Levich, V. G. *Physicochemical Hydrodynamics*; Prentice-Hall: Englewood Cliffs, NJ, 1962.
(66) Wilke, C. R.; Chang, P. *Am. Inst. Chem. Eng. J.* **1955**, *1*, 270.
(67) Rees, N. V.; Klymenko, O. V.; Maisonhaute, E.; Coles, B. A.; Compton, R. G. *J. Electroanal. Chem.* **2003**, *542*, 23.

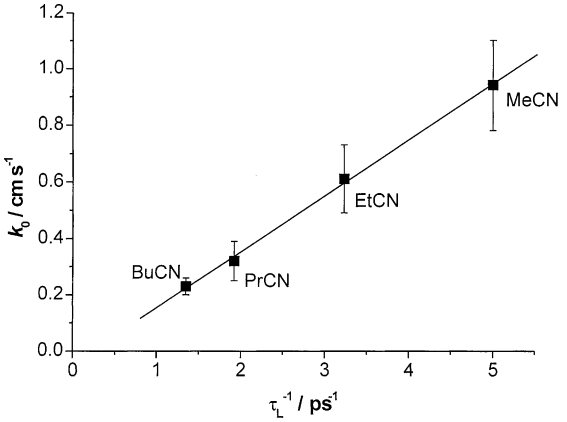

Figure 5. Plot of k_0 vs τ_L^{-1} for DPA in alkyl cyanides (gradient = 1.84×10^{-14}cm; $R^2 = 0.996$).

Table 2. Kinetic Parameters Obtained for the Oxidation of Anthracene Derivatives in Acetonitrile

compound	k_0/cm s^{-1}	α	E_f^0/V (vs Ag)
PA	2.17 ± 0.41	0.51 ± 0.04	1.290 ± 0.003
DPA[62]	0.94 ± 0.16	0.53 ± 0.02	1.400 ± 0.010
CA	1.14 ± 0.09	0.52 ± 0.03	1.513 ± 0.029
DCA	2.00 ± 0.35	0.51 ± 0.01	1.528 ± 0.002
CNA	1.07 ± 0.12	0.51 ± 0.02	1.669 ± 0.003
DCNA	0.68 ± 0.21	0.52 ± 0.04	1.971 ± 0.006
NA	1.07 ± 0.09	0.50 ± 0.01	1.742 ± 0.004
AN	0.94 ± 0.30	0.50	

Plotting the determined vales of k_0 against the reported inverse longitudinal dielectric relaxation times (MeCN = 0.20 ps, EtCN = 0.31 ps, PrCN = 0.52 ps, BuCN = 0.74 ps),[68] we obtain the linear plot with a zero intercept in Figure 5. This is in precise agreement with eq 13, showing that changes in the terms κ_{el}, K_p, and $\Delta G^{\ddagger}$ are either small or compensate each other such that they are not significant on an experimental scale, thus justifiying the assumptions made. This suggests that ν_n is indeed controlled purely by solvent reorganization for this particular system, in common with several others.[31−33] Note that in solvents outside the RCN series, for example, *N*,*N*-dimethylformamide (DMF), the k_0 will not lie on this line, since solvation differences can significantly affect the magnitudes of K_p, κ, and $\Delta G^{\ddagger}$. This is the case for DPA in DMF, where analogous experiments have yielded $k_0 = 0.32 \pm 0.05$ cm s^{-1} which is faster than predicted on the basis of the RCN data.

Oxidation of Anthracene Derivatives in Acetonitrile. To further explore the applicability of this theoretical model to anthracene electron transfer, analogous experiments were conducted for 0.92 mM PA, 0.61 mM CNA, 0.58 mM DCNA, 0.99 mM NA, 1.10 mM CA, and 0.85 mM DCA in MeCN. In all cases, excellent Levich plots were obtained (with $R^2 \geq 0.996$) which yielded values for the respective diffusion coefficients (see Table 3) that were all in good agreement with those predicted by the Wilke−Chang method.[66] The analyses confirmed that these compounds exhibit a simple one-electron oxidation, and the kinetic parameters derived are presented in Table 2 (mean ± standard deviation), with accompanying contour plots shown in the Supporting Information. The values for k_0 vary from 0.68 to 2.17 cm s^{-1}, with no apparent simple explanation. In some cases the disubstituted anthracene has a faster k_0 than the monosubstituted (e.g., DCA vs CA) and others where the opposite is found (e.g., DCNA vs CNA).

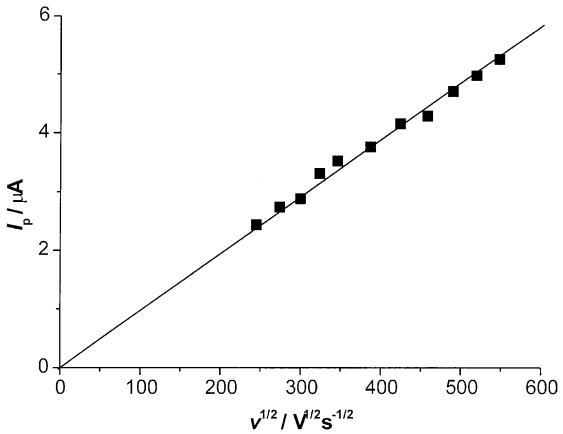

Figure 6. Randles−Sevčik plot for 5.3 mM AN in 0.25 M TBAP/MeCN (gradient = 9.69×10^{-3}; $R^2 = 0.994$).

For comparison purposes, it was attempted to measure the electron transfer for the oxidation of anthracene (AN). However, in this case only, measurement by the HSChE was prevented by slow, slight fouling of the electrode during the course of the experiment. Fast-scan cyclic voltammetry using microdisk electrodes was therefore chosen to record the voltammetry, due to the ease of mechanical cleaning of the electrode during experiments. Experiments were conducted on a solution of 5.3 mM AN in a solution of 0.25 M TBAP and MeCN using a 6.5 μm radius platinum disk electrode, with thorough cleaning (by the method outlined above) carried out between each scan. It was found that at a voltage scan rate of ca. 50 kV s^{-1} there was an approximate peak ratio of 1:1, which was in agreement with literature.[69,70] A series of CVs were then recorded, using full *iR* compensation, at scan rates between 50 and 300 kV s^{-1}, and the peak currents and separations were noted. A plot of the peak currents againt the square root of scan rate yielded a straight line passing through the origin (see Figure 6), which was interpreted in terms of the Randles−Sevčik equation[71]

$$I_p = (2.69 \times 10^5) n^{3/2} \pi r_d^2 D^{1/2} [A]_{bulk} \upsilon^{1/2} \qquad (14)$$

to obtain a value for the diffusion coefficient (at such high voltage scan rates, it is reasonable to approximate the diffusion to the microdisk as planar[72]). A simple *E*-reaction program[73] was then used to simulate peak separations until a match with experiment was was found, and the value of k_0 was noted. This was repeated for each voltammogram (assuming $\alpha = 0.5$) and a mean k_0 reported to be 0.94 ± 0.30 cm s^{-1}. The relatively large standard deviation in this value (32%) compared to that obtained for similar mean k_0 values measured by the HSChE (8−17%) reflects the higher level of precision that the latter method offers.

The interpretation of this result together with the steady-state data require a more detailed consideration of eq 13, as not all of the terms in *A* can be assumed to be invariant to the identity

(68) Krishnaji; Mansingh, A. *J. Chem. Phys.* **1964**, *41*, 827.
(69) Hammerich, O.; Parker, V. D. *Chem. Commun.* **1974**, 245.
(70) Howell, J. O.; Wightman, R. M. *J. Phys. Chem.* **1984**, *88*, 3915.
(71) Bard, A. J.; Faulkner, L. R. *Electrochemical Methods: Fundamentals and Applications*, 2nd ed.; John Wiley: New York, 2001; p 231.
(72) Alden, J. A.; Hutchinson, F.; Compton, R. G. *J. Phys. Chem. B* **1997**, *101*, 949.
(73) Rees, N. V.; Klymenko, O. V.; Compton, R. G.; Oyama, M. *J. Electroanal. Chem.* **2002**, *531*, 33.

of the electroactive compound. First, the free energy of activation can be expressed as a composite of the inner- and outer-sphere reorganization energies, λ_i and λ_o, respectively,[6,7] such that

$$\Delta G^{\ddagger} = \frac{1}{4}(\lambda_i + \lambda_o) \tag{15}$$

For a predominantly outer-sphere electron-transfer process, the major contributor to (15) is the outer-sphere reorganization energy

$$\lambda_o = \frac{N_A e^2}{8\pi\epsilon_0}\left(\frac{1}{r} - \frac{1}{2d}\right)\left(\frac{1}{\epsilon_{op}} - \frac{1}{\epsilon_s}\right) \tag{16}$$

where e is the electronic charge, d is the distance from the reactant to the metal surface (which is usually set to infinity following Hale[74]), ϵ_{op} is the optical permittivity, and ϵ_s is the static permittivity.[14] The value r is the radius of the molecule, which we have taken to be the *hydrodynamic* radius, and can thus be calculated from the Stokes−Einstein equation:[75]

$$r = \frac{kT}{P\pi\eta D} \tag{17}$$

in which η is the viscosity, D is the diffusion coefficient, and P is either 4 or 6 depending whether the "stick" or "slip" limit is assumed for (17).[75] The choice of hydrodynamic radius would appear more attractive than a radius derived from calculations[29,76] or solid-state crystallographic data, since it is directly related to an experimentally measured diffusion coefficient in the reaction solution.[28] However, while calculating the radius in this fashion is convenient, we are nevertheless assuming that the electron transfer is orientation independent. In practice, some weighted average of orientations and their respective "radii" is likely to be relevant. Nevertheless, the hydrodynamic radius should mirror the true effective radius by some factor, and as such will show the correct trend for our interpretation, even if the calculation of the coefficients may be slightly inaccurate.

Second, the κ_{el} term is a measure of the degree of adiabaticity of the electron transfer, which is often assumed to be equal to one.[7] In the case of outer-sphere electron transfer, however, it is known that there is considerably weaker coupling between reactant and electrode leading to nonadiabaticity.[7] Therefore, for nonadiabatic pathways, where $\kappa_{el} < 1$,

$$\kappa_{el} = \kappa_{el}^{\,0} \exp[-B(r' - \sigma)] \tag{18}$$

where r' is the molecule−electrode separation, σ is the distance of closest approach of the molecule and electrode, and B is a constant.[7] For the case of outer-sphere reactions, $r \le r' \le \infty$, and if we rewrite $r' = r + \delta$, then we can express (1) as

$$k_0 = Q\left(\frac{\psi}{4\pi}\right)^{1/2}\left(\frac{1}{r}\right)^{1/2} \exp\left[-\left(Br + \frac{\psi}{r}\right)\right] \tag{19}$$

where

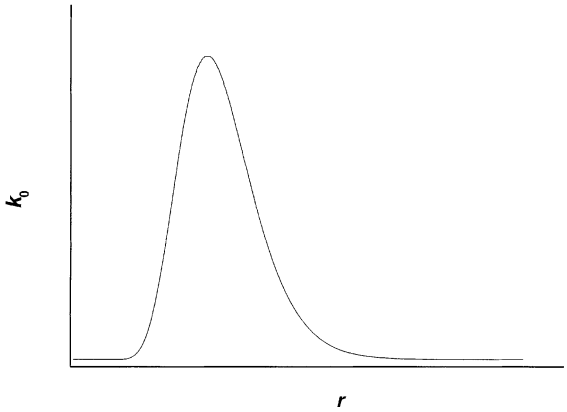

Figure 7. General form for eq 19; k_0 as a function of r. Parameters used for this are $B = 1.5$ Å^{-1} and $Q = 6.00 \times 10^6$cm s^{-1}, being of the same order of magnitude as those found to be experimentally valid.

Table 3. Measured Diffusion Coefficients for Anthracene Derivatives in Acetonitrile, and Hydrodynamic Radii Inferred from the Stokes−Einstein Equation ($P = 4$)'

compound	$D \times 10^5$/cm^2 s^{-1}	r/Å
PA	1.72 ± 0.14	5.35 ± 0.44
DPA[62]	1.40 ± 0.11	6.94 ± 0.54
CA	2.30 ± 0.25	4.07 ± 0.33
DCA	1.98 ± 0.17	4.68 ± 0.37
CNA	2.59 ± 0.25	3.67 ± 0.29
DCNA	1.34 ± 0.10	7.20 ± 0.56
NA	2.39 ± 0.15	3.90 ± 0.31
AN	2.50 ± 0.20	3.75 ± 0.30

$$Q = \frac{K_p \kappa_{el}^{o} \exp[-B(\delta - \sigma)]}{\tau_L}$$

and

$$\psi = \frac{N_A e^2}{32\pi\epsilon_0 RT}\left(\frac{1}{\epsilon_{op}} - \frac{1}{\epsilon_s}\right)$$

This expression suggests a plot of k_0 versus r, the hydrodynamic radius of the molecule, would be meaningful. The form of this expression indicates the plot shown in Figure 7, which undergoes a steep rise before passing through a maximum and rapidly decaying toward zero.

The heterogeneous rate constants measured in MeCN have been plotted against their hydrodynamic radii, the values for which are given in Table 3, having been calculated from eq 17 using the "slip" limit of $P = 4$. This shows a maximum in the rate constant, at an optimal value of r, with lower values of k_0 for lower and higher radii. This shape is analogous to that of eq 19, but it is simpler to fit the experimental data using a linearized form of the above equation, which for convenience can be rendered dimensionless by making the substitutions $y = r/\psi$, $\beta = \psi B$, and introducing a arbitrary rate constant of $k' = 1$ cm s^{-1}, and setting $K = k_0/k'$ and $q = Q/k'$. Equation 19 then can be written as

$$K = \left(\frac{q}{2\sqrt{\pi}}\right)\left(\frac{1}{y}\right)^{1/2} \exp\left[-\left(\beta y + \frac{1}{y}\right)\right] \tag{20}$$

and hence

(74) Hale, J. M. In *Reactions of Molecules at Electrodes*; Hush, N. S., Ed.; Wiley: London, 1971; p 243.
(75) Bockris, J. O'M.; Reddy, A. K. N. *Modern Electrochemistry 1: Ionics*, 2nd ed.; Plenum Press: New York, 1998.
(76) Kapturkiewicz, A.; Jaenicke, W. *J. Chem. Soc., Faraday Trans. 1* **1987**, *83*, 2727.

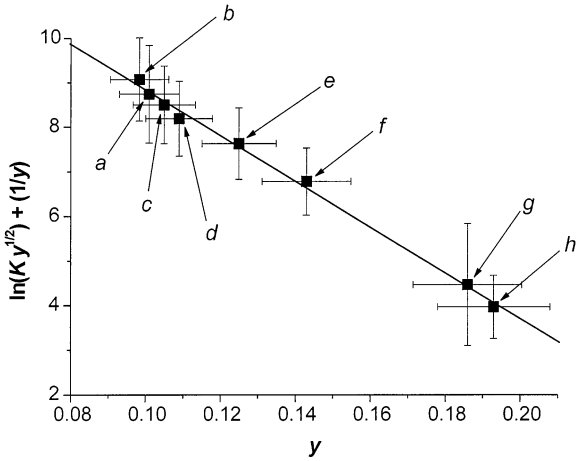

Figure 8. Best fit plot of $[\ln(K(y)^{1/2}) + 1/y]$ vs y for the anthracene derivatives in MeCN. Concentrations are as given in the text and the compounds are numbered as follows: (a) AN, (b) CNA, (c) NA, (d) CA, (e) DCA, (f) PA, (g) DPA, (h) DCNA.

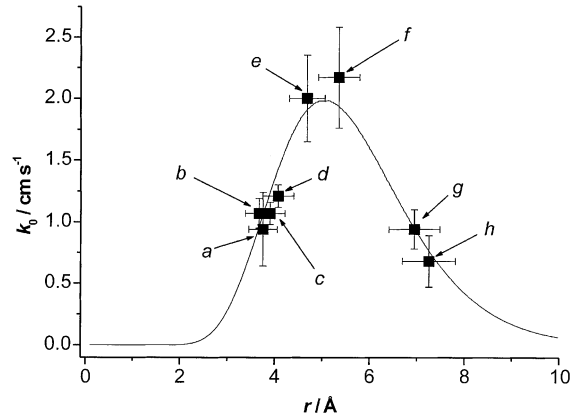

Figure 9. Plot of k_0 vs r for anthracene derivatives in MeCN using the values $B = 1.37$ Å^{-1} and $Q = 4.00 \times 10^6$cm s^{-1} derived above from the linear plot in Figure 8 for the optimum fit of the data. The concentrations are as given in the text and the compounds are numbered as follows: (a) AN, (b) CNA, (c) NA, (d) CA, (e) DCA, (f) PA, (g) DPA, (h) DCNA.

$$\ln(K\sqrt{y}) + \frac{1}{y} = -\beta y + \ln\left(\frac{q}{2\sqrt{\pi}}\right) \qquad (21)$$

This graph is shown in Figure 8 and yields a linear plot with a gradient of 51.06 and $R^2 = 0.996$. From this plot, values of Q and B can be extracted using the known value for ψ of 37.3 Å. This gives $B = 1.37$ Å^{-1} and $Q = 4.00 \times 10^6$ cm s^{-1}. These values are physically reasonable, as B values have been reported[7,77] to range typically from 1 to 2 Å^{-1}. These values can then be input into the original formula (19) to visualize the direct relationship between k_0 and r, as shown in Figure 9. It should be noted that in the above analysis no account has been taken of double layer effects.[7,11]

By implication, given the assumptions and approximations made above, the maximum rate constant for the oxidation of a similar anthracene molecule in acetonitrile would be around 2.0−2.3 cm s^{-1}, which would correspond to a hydrodynamic radius of ca. 5.1 Å. To the best knowledge of the authors, this is the first attempt to rationalize the trends in k_0 among a series of related compounds within the same solvent using this theoretical framework in which the hydrodynamic radii are used for the molecular dimension (r) appearing in eq 19. The results show an excellent correlation between the experimentally determined heterogeneous electron-transfer rate and the function generated from the Marcus eq 19, thus suggesting that the hydrodynamic radius is the appropriate measure of molecular size for this context.

Conclusions

The HSChE has been used to measure *fast* heterogeneous electron-transfer rates under steady-state conditions, thereby avoiding the problems of charging currents and *iR* losses. This has enabled a *quantitative* assessment of Marcus Theory to be made with confidence in the experimental data. Specifically, the dependence of k_0 on both the solvent longitudinal dielectric relaxation (τ_L) and hydrodynamic radius (r) have been investigated separately and the results from theoretical models verified.

Acknowledgment. We appreciate the generosity of Professor C. Amatore and Dr. E. Maisonhaute in making available to us the designs for the fast-scan potentiostat apparatus developed in their laboratory. We thank the EPSRC for a studentship and Avecia Ltd. for CASE support for N.V.R. and the Clarendon Fund for partial funding for O.V.K.

Supporting Information Available: Contour plots showing k_0, E_f^0, α, as they vary independently with MSAD for the oxidation of anthracene derivatives in MeCN. The plots have single minima, corresponding to the unique set of optimized values. The compounds shown are PA, CA, DCA, CNA, DCNA, and NA. This material is available free of charge via the Internet at http://pubs.acs.org.

JA040014V

(77) Logan, J.; Newton, M. D. *J. Chem. Phys.* **1983**, *78*, 4086.